



Engineering Notes

Spatial Dynamics and Control of a Two-Craft Coulomb Formation

Vladimir S. Aslanov*

Samara National Research University, 443086, Samara, Russia

DOI: 10.2514/1.G004382

Nomenclature

a_p	=	acceleration of the space tug, m/s^2
C_1xyz	=	hill-frame
$C_2x_2y_2z_2$	=	space debris frame
c_d	=	feedback control coefficient, $1/s^2$
\dot{c}_d	=	feedback control coefficient, $1/s$
c_α, c_β	=	feedback control coefficient, m/s^2
$\dot{c}_\alpha, \dot{c}_\beta$	=	feedback control coefficient, m/s
d	=	center-to-center separation distance of the tug and debris
$F_{E,i}$	=	Coulomb force, N
G	=	angular momentum projection on the line C_1C_2 divided by transverse inertia moment of the space debris, $1/s$
J	=	transverse inertia moment of the space debris, $kg \cdot m^2$
(J_x, J_y, J_z)	=	moments of inertia of the space debris, $kg \cdot m^2$
\mathbf{K}	=	angular momentum vector
k_c	=	Coulomb's constant, $8.99 \cdot 10^9 (N \cdot m^2)/C^2$
l	=	distance between the mass center of the space debris and Coulomb forces application points, m
m_1	=	mass of the tug, kg
m_2	=	mass of the debris, kg
n	=	mean orbital rate of the space tug, $1/s$
\mathbf{P}	=	tug's thrust force, N
R	=	angular momentum projection on the symmetry axis of the space debris divided by transverse inertia moment, $1/s$
U_x, U_y, U_z	=	projections of the control force, N
u_x, u_y, u_z	=	projections of the control accelerations, m/s^2
Φ_i	=	craft voltages, V
(α, β)	=	spherical angles
(θ, ψ)	=	pitch, roll angles
θ_s	=	stable equilibrium position of the pitch angle

I. Introduction

SPACE debris is a growing concern for both low-Earth-orbit (LEO) and geosynchronous orbit (GEO) regimes [1–3]. The defunct GEO satellites tend to be very large, often reaching beyond 5–10 m in size, as well as rotating and tumbling [4]. The act of

docking onto such large and tumbling space objects is very challenging; as a result, novel touchless debris removal or despinning solutions are being explored. The ion shepherd method uses the ion engine exhaust to push and/or despin a satellite [5], whereas the laser ablation method uses the debris' own mass as a thruster fuel source [6,7]. A promising touchless and low-power solution is the electrostatic tractor [8]. Most of the control research using the electrostatic tractor considers a pulling configuration to move GEO objects [9]. A feedback control law is proposed that stabilizes the relative motion of the space tug and space debris during active debris removal using the Coulomb force for the push scheme [10]. In Ref. [11] the pusher configuration is considered with taking into account an attitude motion. An influence of flexible appendages on satellite attitude motion in the Coulomb interaction is studied for the pusher configuration [12]. Moreover, equations of spatial attitude motion in the canonical form are deduced, and exact solutions are obtained using Jacobi elliptic functions, in the case where the distance between the space debris and the tug remains unchanged. If the distance and voltage change slowly over time, adiabatic invariants are found in terms of the complete elliptic integrals [13].

The aim of this Note is to generate a feedback control law of the space tug and debris for the removal and detumbling of the space debris or defunct satellites using electrostatic forces. The goal is to provide a stable relative motion of the tug and the debris, in terms of both translation and rotation. With the spacecraft and debris nominally charged with the same polarity to consider a pusher configuration, a feedback control method using both the thrusters for station-keeping and the electrostatic charge modulation of the space tug for pushing and detumbling is considered. The feedback control laws align the tug–debris direction with the tug along track orbit axis and maintain a nominally constant distance between the charged tug and debris, all while stabilizing the attitude motion of the debris. Note that if the debris has the shape of a ball, then there is no need to stabilize its attitude motion when towing, because the electrostatic forces of interaction between the bodies (debris and tug) do not depend on the angular position of the debris. If the debris has an elongated shape, for example, as an upper stage or a geostationary communication satellite with large solar panels, then due to its oscillations or rotation, the electrostatic forces will vary according to a periodic law, causing a variable relative acceleration and a change of the distance between the bodies. Further, because of this, the electrostatic forces will also change. And in this case, an undesirable self-oscillation mode may occur. And second, due to the potential difference between the bodies, the possibility of a short circuit increases for the rotating or oscillating elongated debris.

The feature of this study is that it considers a translational motion of the center of mass of the debris relative to the tug in the 3-D frame (three degrees of freedom: d, α, β ; Fig. 1) and the spatial attitude motion (or in other words: rotational motion) of the debris (three degrees of freedom—three Euler angles: pitch θ , precession (roll) ψ , and spin φ ; Fig. 1) as a rigid body relative to its own center of mass. The roll angle does not affect the rotational motion of the axisymmetric body (debris) and therefore will not be further considered. The rotational motion of the debris is very different from the planar motion one in that the mechanical principles valid for the plane motion do not work in this case. First, according to Eqs. (6–11) from [13], the pitch angle θ can never be equal to zero. Second, the stable position depends on the values of the generalized momentums [in our case, R and G in Eqs. (10) and (11)] and only in the particular case it can be equal to the value $\theta = \pi/2$, as in the case of the plane motion, when $R = 0$ and $G = 0$. The stable position of the rotational motion θ_s completely depends on the initial position of the tug relative to the debris and the vector of the angular momentum of the debris.

Received 2 February 2019; revision received 3 July 2019; accepted for publication 6 August 2019; published online 5 September 2019. Copyright © 2019 by the American Institute of Aeronautics and Astronautics, Inc. All rights reserved. All requests for copying and permission to reprint should be submitted to CCC at www.copyright.com; employ the eISSN 1533-3884 to initiate your request. See also AIAA Rights and Permissions www.aiaa.org/randp.

*Head, Theoretical Mechanics Department, 34 Moskovskoe shosse; aslanov_vs@mail.ru.

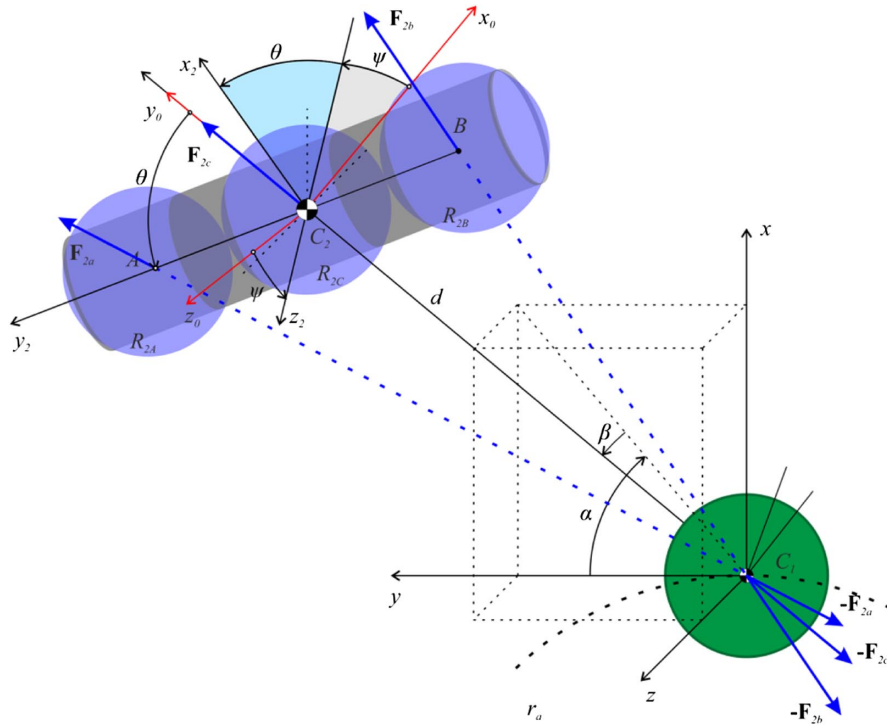


Fig. 1 The three-sphere model, frames, forces, coordinates.

Only in the particular case, it is possible to achieve that the debris is located perpendicular to the line connecting the mass centers of the debris and the tug. Based on physical nature of the rotational motion of the debris under the action of electrostatic forces, an original mathematical model is proposed for analyzing the initial system configuration and a numerical simulation. We show that the rotational motion of the debris as the axisymmetric rigid body under the action of electrostatic forces is analogous to the Lagrange case of the heavy top. The proposed mathematical model allows, first, to carry out a detailed analytical analysis of the effect of the initial configuration of the tug–debris system on its motion and, second, to study in detail the controlled motion of the system as a whole.

The Note is structured as follows: First, the fundamentals of relative dynamics with respect to a slowly accelerating Hill frame and the 3-D motion equations of the debris as a rigid body are provided. The relative dynamics of the two body in the rotating Hill frame are developed considering electrostatic and thruster effects. Next, a spherical coordinate frame is introduced and then is used to develop a feedback control law. The feedback control law aligns the tug–debris direction with the tug along track orbit axis and maintains a nominally constant distance between the charged tug and debris, all while stabilizing the attitude motion of the debris. A method for determining the initial configuration of the tug–debris system is proposed to ensure the position of the debris required for towing. Finally, numerical simulation is used to illustrate the feedback control laws in maintaining the desired position of the tug–debris system.

II. Mathematical Models

A. Description of the System

The tug is assumed to be a sphere with a homogenous potential, and the debris is assumed as a rigid conducting cylindrical dynamically symmetric body that has nominal electric charges of the same sign; the repulsive electrostatic forces act between the tug and the debris. Furthermore, the tug has three thrusters: the main thruster, which provides the acceleration of the whole system for the disposal of the debris to a disposal orbit, and two control thrusters, which ensure the required position of the tug relative to the debris. The thrusters are directed mutually perpendicular. The magnitude of the thrust force they create may vary independently.

We consider the in-space motion only. There are three coordinate frames that are used to describe the motion of the mechanical system throughout this Note (Fig. 1).

The rotating local-vertical-local-horizontal (LVLH), often also referred to as the Hill coordinate frame C_1xyz , has its origin coincide with the tug center of mass C_1 . Axis C_1x is aligned with the local vertical line, the C_1y axis is aligned with the local horizontal line, and axis C_1z makes the frame right-handed [14].

The intermediate frame $C_2x_0y_0z_0$ has the debris's origin at the center of mass C_2 . The relative orientation angles α and β θ are the angle sequence with respect to the Hill frame C_1xyz . Carrying out the matrix multiplication leads to the direction cosine matrix mapping from the Hill frame to the spherical frame $C_2x_0y_0z_0$:

$$A_1 = A_\alpha \cdot A_\beta = \begin{bmatrix} \cos \alpha & \sin \alpha & 0 \\ -\sin \alpha & \cos \alpha & 0 \\ 0 & 0 & 1 \end{bmatrix} \cdot \begin{bmatrix} 1 & 0 & 0 \\ 0 & \cos \beta & -\sin \beta \\ 0 & \sin \beta & \cos \beta \end{bmatrix} \quad (1)$$

The debris frame $C_2x_2y_2z_2$ also has the origin at the center of mass C_2 of the debris. Axis C_2y_2 directs along the longitudinal axis of symmetry the cylindrical debris. The connection between the frames $C_2x_0y_0z_0$ and $C_2x_2y_2z_2$ occurs through the two Euler angles (θ, ψ) —pitch and roll angles.

$$A_2 = A_\psi \cdot A_\theta = \begin{bmatrix} \cos \psi & 0 & \sin \psi \\ 0 & 1 & 0 \\ -\sin \psi & 0 & \cos \psi \end{bmatrix} \cdot \begin{bmatrix} \cos \theta & -\sin \theta & 0 \\ \sin \theta & \cos \theta & 0 \\ 0 & 0 & 1 \end{bmatrix} \quad (2)$$

For the dynamically axisymmetric debris ($J_x, J_y, J_z = J_x$), the third Euler angle (roll) does not make sense to introduce, because the attitude motion of the body does not depend on it.

B. Multisphere Model Overview

According to Ref. [15] the multi-sphere method is a means to approximate the electrostatic interactions between conducting objects with generic geometries. Figure 1 depicts a cylindrical satellite, modeled by three spheres [15]. Both objects are assumed for now to be conducting and reside at voltage levels Φ_1 and Φ_2 . Because voltages Φ_i

are assigned to the craft, technically the charge q_i on each sphere depends on the voltage [15]. This relation is governed by Eq. (4) [15], where R_i represents the radius of the sphere in question and $r_{i,j} = r_j - r_i$ is the center-to-center distance to each neighbor. The constant $k_c = 8.99 \cdot 10^9 \text{ (N} \cdot \text{m}^2)/\text{C}^2$ is Coulomb's constant.

$$\Phi_i = k_c \frac{q_i}{R_i} + \sum_{j=1, j \neq i}^m k_c \frac{q_j}{r_{i,j}} \quad (3)$$

These relations can be combined for each sphere to obtain the matrix equation

$$\begin{bmatrix} \Phi_1 \\ \Phi_2 \\ \Phi_2 \\ \Phi_2 \end{bmatrix} = k_c [C_M]^{-1} \begin{bmatrix} q_1 \\ q_a \\ q_c \\ q_b \end{bmatrix} \quad (4)$$

where

$$[C_M]^{-1} = \begin{bmatrix} 1/R_1 & 1/r_a & 1/r_c & 1/r_b \\ 1/r_a & 1/R_{2,a} & 1/l & 1/2l \\ 1/r_b & 1/l & 1/R_{2,c} & 1/l \\ 1/r_c & 1/2l & 1/l & 1/R_{2,b} \end{bmatrix} \quad (5)$$

where R_1 is the radius of the tug.

By inverting $[C_M]^{-1}$, the charge on each sphere is determined at any instance of time. The charge redistribution and interaction with the space environment are assumed to be orders of magnitude faster than the spacecraft motion.

The total electrostatic force is then given by the summations [15]

$$\mathbf{F}_{E2} = -\mathbf{F}_{E1} = k_c |q_1| \sum_{i=a}^c \frac{q_i}{r_i^3} \mathbf{r}_i \quad (6)$$

and for each of the three spheres of object 2

$$\mathbf{F}_{2i} = k_c \frac{|q_1| q_i}{r_i^3} \mathbf{r}_i, \quad (i = a, b, c) \quad (7)$$

$$\mathbf{r}_a = \mathbf{r}_c + A \cdot \begin{bmatrix} 0 \\ l \\ 0 \end{bmatrix}, \quad \mathbf{r}_b = \mathbf{r}_c + A \cdot \begin{bmatrix} 0 \\ -l \\ 0 \end{bmatrix}, \quad (8)$$

$$\mathbf{r}_c = A_1 \cdot \begin{bmatrix} 0 \\ d \\ 0 \end{bmatrix}$$

$$A = A_1 \cdot A_2 \quad (9)$$

where l is distance between the points C_2 and A (or B), and d is center-to-center separation distance of the tug and debris (Fig. 1).

C. Spatial Motion Equations of the Debris

Let us study the motion of the debris under the action of the Coulomb force only and do not take into account other forces and torques. To describe the motion of the debris relative to its own mass center C_2 , we use the angular momentum theorem [13]

$$\ddot{\theta} + \frac{(G - R \cos \theta)(R - G \cos \theta)}{\sin^3 \theta} = \frac{1}{J} L_\theta \quad (10)$$

$$\dot{\psi} = \frac{(G - R \cos \theta)}{\sin^2 \theta} \quad (11)$$

where (J, J_y, J_z) are moments of inertia of the debris in the frame $C_2x_2y_2z_2$, and G and R are up to a factor of the vector angular momentum projections on the C_2y_0 and C_2y_2 , respectively:

$$G = \frac{K_\psi}{J} = \text{const}, \quad R = \frac{K_\phi}{J} = \text{const} \quad (12)$$

Note that the electrostatic torque is determined by electrostatic forces (7), which acts only in the nutation plane; therefore

$$L_\theta = \begin{bmatrix} 0 \\ 0 \\ 1 \end{bmatrix} \cdot \mathbf{L}_\theta, \quad (13)$$

$$\mathbf{L}_\theta = \begin{bmatrix} 0 \\ l \\ 0 \end{bmatrix} \times (A^T \cdot \mathbf{F}_{2a}) + \begin{bmatrix} 0 \\ -l \\ 0 \end{bmatrix} \times (A^T \cdot \mathbf{F}_{2b})$$

$$A^T = (A_1 \cdot A_2)^T \quad (14)$$

D. Spatial Attitude Equations of the Debris

The LVLH frame is a noninertial frame C_1xyz , and so the equations of the debris relative to the space tug contain the terms associated with the motion of the LVLH frame relative to the Earth. The equation has the classical form [14]

$$\begin{aligned} \ddot{x} - 2n\dot{y} - 3n^2x &= a_x \\ \ddot{y} + 2n\dot{x} &= a_y \\ \ddot{z} + n^2z &= a_z \end{aligned} \quad (15)$$

where n is the orbital rate of the space tug, which is changed under the action of the tug's thrust. The change of the orbital rate \dot{n} is approximated as

$$\dot{n} = \frac{P}{m_1 + m_2} \frac{1}{r} \quad (16)$$

where r is the distance from the Earth center to the center of mass of the system. The rate of change of n is close to 0 due to small value of the thrust force P , and so the value of \dot{n} is neglected [16]. For example, electric thrusters have thrust output in the micro- to millinewton range. For $P = 20 \text{ mN}$ and $m_1 + m_2 = 5000 \text{ kg}$

$$\dot{n} = \frac{20 \text{ mN}}{5000 \text{ kg}} \cdot \frac{1}{35786 \text{ km}} \approx 10^{-13} \text{ s}^{-2} \quad (17)$$

This value is several orders of magnitude smaller than the magnitude of $n^2 \approx 5 \cdot 10^{-9} \text{ 1/s}^2$ presented in Eqs. (15).

The right side of Eqs. (15) includes projections of the acceleration produced by the main thruster and control thrusters of the tug and by the electrostatic force

$$\mathbf{a} = \begin{bmatrix} a_x \\ a_y \\ a_z \end{bmatrix} = -\mathbf{F}_{E1} \left(\frac{m_1 + m_2}{m_1 m_2} \right) - (\mathbf{a}_P + \mathbf{u}_x + \mathbf{u}_y + \mathbf{u}_z) \quad (18)$$

where \mathbf{a}_P is the acceleration of the space tug provided by the main engine thrust P

$$\mathbf{a}_P = \frac{P}{m_1} \begin{bmatrix} 0 \\ 1 \\ 0 \end{bmatrix} = \begin{bmatrix} 0 \\ a_P \\ 0 \end{bmatrix} \quad (19)$$

u_x, u_y, u_z are the accelerations created by the control engines U_x, U_y, U_z

$$u_x = U_x/m_1, \quad u_y = U_y/m_1, \quad u_z = U_z/m_1 \quad (20)$$

The longitudinal coordinate y of the debris relative to the tug should be equal to the required distance between these objects, and the transverse coordinates x and z should be zero in the process of towing (Fig. 1). To stabilize the relative distance between the debris and tug, we apply the control laws from Ref. [10] using the same control structure for the transverse coordinates:

$$u_x = c_\alpha \sin \alpha + c_{\dot{\alpha}} \dot{\alpha} \quad (21)$$

$$u_y = c_d(d - d_s) + c_{\dot{d}} \dot{d} \quad (22)$$

$$u_z = c_\beta \sin \beta + c_{\dot{\beta}} \dot{\beta} \quad (23)$$

where $c_k, c_{\dot{k}}$ are control coefficients ($k = \alpha, \beta, d$), and d_s is the given distance between the space tug and debris.

III. Stability of Charged Closed-Loop Attitude Motion

The next step is to choose the attitude control law to stabilize the spatial attitude motion of the debris. Only the magnitude electric charge of the tug can affect the attitude motion of the debris. However, in this case, the control law of the electrical change tug proposed for plane motion and given as Eq. (76) from Ref. [11]

$$\Phi_1 = \bar{\Phi}_1(1 + \kappa \dot{\theta} \sin 2\theta) \quad (24)$$

cannot be used. The desired stable equilibrium position of the debris as a cylinder is a position in which its longitudinal axis is perpendicular to the line connecting the centers of mass of the bodies; that is,

$$\theta_s = \frac{\pi}{2} \quad (25)$$

where θ_s is stable equilibrium position of the pitch attitude angle.

In the general case of the spatial motion ($R \neq 0, G \neq 0$), then, as follows from Eq. (10), the equilibrium position differs from Eq. (25) and can be equal to $\pi/2$ only if

$$R = 0, \quad G = 0 \quad (26)$$

Therefore, when using the control law of the electrical change tug (24) the pitch attitude angle θ cannot be reduced to the equilibrium position (25).

Consider the procedure for the approximate determination of the equilibrium position of the debris. Assuming that the distance between the tug and debris is considerably greater than the distance between the mass center of the space debris and Coulomb forces application points (Fig. 1)

$$\lambda = \frac{l}{d} \ll 1 \quad (27)$$

then the electrostatic moment can be approximated by the following function [12,15,17,18]

$$L_\theta = bJ_y \sin 2\theta \quad (28)$$

In this case, Eq. (10) is rewritten as

$$\ddot{\theta} + \frac{(G - R \cos \theta)(R - G \cos \theta)}{\sin^3 \theta} - b \sin 2\theta = 0 \quad (29)$$

One can easily see the similarity of Eq. (29) and the equation motion of a symmetric heavy top (classical case of Lagrange) Eq. (4.68) in Ref. [19]

$$\ddot{\theta} + \frac{(G - R \cos \theta)(R - G \cos \theta)}{\sin^3 \theta} + b \sin \theta = 0 \quad (30)$$

where $b = \text{const} > 0$.

By analogy with the Lagrange case, the equilibrium position $\theta = \theta_s$ of Eq. (29) is the root of the following equation:

$$\frac{(G - R \cos \theta_s)(R - G \cos \theta_s)}{\sin^3 \theta_s} - b \sin 2\theta_s = 0 \quad (31)$$

Of course, all of the above can be applied to the original Eq. (10), converting the first and second derivatives to zero.

As a result of this discussion, the control law of the electrical change tug for the spatial motion can be written as

$$\Phi_1 = \bar{\Phi}_1[1 + \kappa \dot{\theta} \sin 2(\theta - \theta_s)] \quad (32)$$

where κ is a constant coefficient, $\bar{\Phi}_1 = \text{const} < 0$.

It is now clear that the law (32) is aimed only at the realization of the stable equilibrium position of the debris $\theta \rightarrow \theta_s$. Another equally important task is to choose the initial position of the tug relative to the debris and its initial attitude motion, which would ensure the required values of parameters R, G , and b , consequently, and θ_s .

IV. Simplified Nonlinear Model

The very complicated forms of the formulas for the forces in Eq. (7) and the electrostatic torque in Eq. (13) due to the presence of vector-matrix transformations (1–5) make their practical use very difficult. The following assumptions are used to simplify these formulas, and hence the equations of motion described in Eqs. (10) and (15). So, assume that the distance between the tractor and debris is considerably greater than the distance between the mass center of the space debris and Coulomb forces application points (27). Using the assumption (27) the electrostatic torque (13) is represented as

$$L_\theta = \lambda^3 \frac{R_1 \Phi_1}{2k_c} \sin 2\theta \left(3\Phi_2 + \frac{R_1}{d} \Phi_1 \right) \quad (33)$$

The Cartesian coordinates (x, y, z) are replaced by new the spherical coordinates (d, α, β)

$$d = \sqrt{x^2 + y^2 + z^2} \quad (34)$$

$$\alpha = \arctan\left(\frac{x}{y}\right) \quad (35)$$

$$\beta = \arcsin\left(\frac{-z}{d}\right) \quad (36)$$

and

$$\begin{bmatrix} x \\ y \\ z \end{bmatrix} = A_1 \cdot \begin{bmatrix} 0 \\ d \\ 0 \end{bmatrix} = \begin{bmatrix} \cos \alpha & \sin \alpha \cos \beta & -\sin \alpha \sin \beta \\ -\sin \alpha & \cos \alpha \cos \beta & \cos \alpha \sin \beta \\ 0 & \sin \beta & \cos \beta \end{bmatrix} \quad (37)$$

Taking into account the change of variables (37) and Eqs. (21–23) and (33), we rewrite Eqs. (15), (10), and (11) in the following form:

$$\ddot{\alpha} = \frac{l^3 R_1 \Phi_1 (R_1 \Phi_1 + 3d\Phi_2)}{2k_c m_* d^6} \sin 2\theta \cos \psi \sec \beta + \frac{1}{2d} [2(a_1 - u_y) \sin \alpha \sec \beta + 3dn^2 \sin 2\alpha + 2u_x \cos \alpha \sec \beta - 4\dot{\alpha}(\dot{\alpha} - n)] + 2(\dot{\alpha} - n)\dot{\beta} \tan \beta \quad (38)$$

$$\ddot{\beta} = -\frac{l^3 R_1 \Phi_1 (R_1 \Phi_1 + 3d\Phi_2)}{2k_c m_* d^6} \sin 2\theta \sin \psi + \frac{1}{2d} [2(a_1 - u_y) \cos \alpha \sin \beta - 2u_x \sin \alpha \sin \beta + 2u_z \cos \beta - 4\dot{\beta}] + \frac{1}{4} (-5n^2 + 3n^2 \cos 2\alpha + 4n\dot{\alpha} - 2\dot{\alpha}^2) \sin 2\beta \quad (39)$$

$$\ddot{d} = (-a_1 + u_y) \cos \alpha \cos \beta + \frac{dn^2}{4} (1 - 6 \cos 2\alpha \cos^2 \beta + 5 \cos 2\beta) + u_x \sin \alpha \cos \beta + u_z \sin \beta + d(\dot{\alpha} - 2n)\dot{\alpha} \cos^2 \beta + d\dot{\beta}^2 + \frac{lR_1 \Phi_1 (R_1 \Phi_1 - d\Phi_2)}{64k_c m_* d^3 R_{2,b} R_{2,c}^2} [9lR_{2,b}(l + 4R_{2,c}) - 16lR_{2,c}(3l - 2R_{2,c}) - 112R_{2,b}R_{2,c}^2] \quad (40)$$

$$\ddot{\theta} + \frac{(G - R \cos \theta)(R - G \cos \theta)}{\sin^3 \theta} = \frac{l^3 R_1 \Phi_1}{2k_c J d^3} \sin 2\theta \left(3\Phi_2 + \frac{R_1}{d} \Phi_1 \right) \quad (41)$$

$$\dot{\psi} = \frac{(G - R \cos \theta)}{\sin^2 \theta} \quad (42)$$

where $m_* = (m_1 m_2 / m_1 + m_2)$, $a_1 = (P / m_1)$, $\Phi_1 = \bar{\Phi}_1 [1 + \kappa \theta \sin 2(\theta - \theta_s)]$.

V. Choice of the Initial Position of the Tug

Let us find out how the tug position relative to the debris at the moment of switching on the Coulomb interaction affects the attitude motion of the debris. Free attitude motion of the axisymmetric debris before the beginning of the Coulomb interaction with the tug is characterized by a constant (in magnitude and direction), the angular momentum vector \mathbf{K} . Before the beginning of the coulomb interaction, external moments acting on the debris are absent, including with respect to the symmetry axis of the debris $C_2 y_2$; therefore, the projection of the angular momentum vector \mathbf{K} on the axis $C_2 y_2$ and the angle γ between this axis and the angular momentum vector \mathbf{K} are constant; that is,

$$JR = K \cos \gamma = \text{const} \rightarrow \gamma = \text{const} \quad (43)$$

One can find out where the tug should be at the beginning of the electrostatic interactions relative to the symmetry axis of the debris $C_2 y_2$ and the angular momentum vector \mathbf{K} . Let at the initial moment the debris is in the state of equilibrium and rest:

$$\ddot{\theta} = 0, \quad \dot{\theta} = 0, \quad \theta = \theta_s, \quad d = d_s \quad (44)$$

then Eq. (41) takes the form

$$\frac{(G - R \cos \theta_s)(R - G \cos \theta_s)}{\sin^3 \theta_s} - b \sin 2\theta_s = 0 \quad (45)$$

where

$$b = \frac{l^3 R_1 \bar{\Phi}_1}{2k_c J d_s^4} (3d_s \Phi_2 + R_1 \bar{\Phi}_1) \quad (46)$$

Solving Eq. (45) relative to G obtains

$$G = \left(R + \frac{b}{R} \right) \cos \theta_s \quad (47)$$

Hence, it is clear that if we want to get the equilibrium position

$$\theta_s = \frac{\pi}{2} \quad (48)$$

then the tug relative to the debris should be positioned so that by virtue of Eq. (12) we get

$$G = \frac{K}{J} \cos \eta = 0 \quad (49)$$

Therefore, the angle between the line $C_1 C_2$ and the angular momentum vector \mathbf{K} should be equal to (Fig. 2)

$$\eta = \frac{\pi}{2} \quad (50)$$

To simultaneously satisfy the conditions (48) and (49), line $C_1 C_2$ must be perpendicular to the plane formed by the angular momentum vector \mathbf{K} and the symmetry axis of the debris $C_2 y_2$.

Thus, we have found the “ideal” initial conditions at the moment of switching on the electric charge in the form:

$$\theta_0 = \frac{\pi}{2}, \quad \dot{\theta}_0 = 0, \quad d_0 = d_s, \quad \dot{d}_0 = 0, \quad G = 0 \quad (51)$$

In reality, for example, deviations of the initial pitch attitude angle can occur

$$\theta_0 = \frac{\pi}{2} \pm \Delta\theta_0 \quad (52)$$

In this case, control (32) will also lead the debris to the equilibrium position (48), but this may require a large electrical voltage.

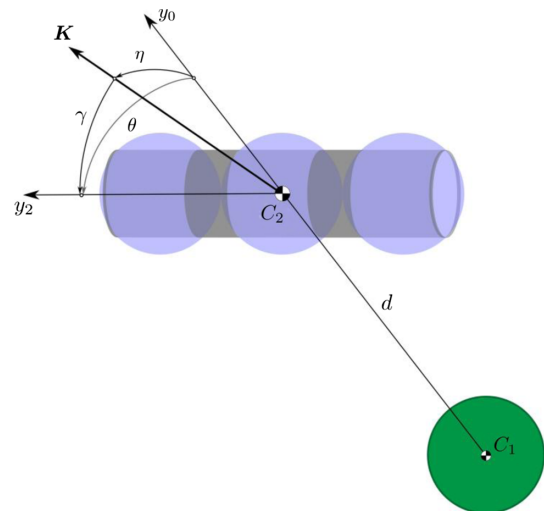


Fig. 2 Initial position of the tug position relative to the debris.

Table 1 Simulation parameters for the detumble control scenario

Parameter	Value
J , $\text{kg} \cdot \text{m}^2$	50
$\Phi_2 = \Phi_1 $, kV	25
R_1 , m	0.5
$R_{2,a} = R_{2,b}$, m	0.59
$R_{2,c}$, m	0.65
l , m	0.5
m_1 , kg	500
m_2 , kg	1000
P , mN	10

VI. Numerical Simulation

This section shows with numerical simulations how the initial configuration of the tug–debris system and the proposed feedback control affect the stability of the system. In all cases the control goal is to reduce the debris tumble rate (i.e., $\dot{\theta} \rightarrow 0$, $\theta \rightarrow \theta_s$) and keep the spacecraft aligned in a leader–follower configuration (i.e., $\alpha = 0$, $\dot{\alpha} = 0$, $\beta = \beta = 0$) and at a given distance (i.e., $d = d_s$). The investigation is performed by numerical integration of the motion equations in Eqs. (38–42) for the control law Eqs. (21–23) and (32). For numerical simulations, system parameters are chosen as in Table 1. The sizes and locations of the spheres are taken from paper [17].

Additional simulation parameters of the system are given in Table 2.

The magnitude of the angular momentum and the angle between the vector of the angular momentum and the symmetry axis of the debris for all variants are taken equal to

$$K = 10 \text{ kg} \cdot \text{m}^2 \cdot \text{s}^{-1} \quad (53)$$

$$\gamma = \frac{\pi}{6} \quad (54)$$

then we obtain

$$R = \frac{K \cos \gamma}{J} = 0.1 \text{ s}^{-1} \quad (55)$$

The differential Eqs. (38–40) and (42) are integrated with the following initial conditions:

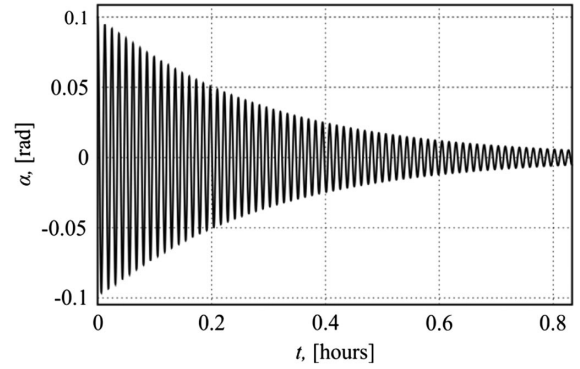
$$\begin{aligned} \alpha_0 = 0.1, \quad \dot{\alpha}_0 = 0 \text{ s}^{-1}, \quad \beta_0 = 0.1, \quad \dot{\beta}_0 = 0 \text{ s}^{-1}, \\ d_0 = d_s, \quad \dot{d}_0 = 0.1 \text{ m} \cdot \text{s}^{-1}, \quad \psi_0 = 0 \end{aligned} \quad (56)$$

Consider four cases of the initial motion conditions for the attitude motion equation of the debris (41).

Case 1: The “ideal” initial conditions for Eq. (41), with Eqs. (51–54) taken into account, are written as

Table 2 Numerical simulation parameters

Parameter	Value
d_s , m	5
κ , s^{-1}	−20
b , s^{-2}	0.00003
c_α , $\text{m} \cdot \text{s}^{-2}$	−0.1
$c_{\dot{\alpha}}$, $\text{m} \cdot \text{s}^{-1}$	−0.01
c_β , $\text{m} \cdot \text{s}^{-2}$	−0.1
$c_{\dot{\beta}}$, $\text{m} \cdot \text{s}^{-1}$	−0.01
c_d , $\text{m} \cdot \text{s}^{-2}$	−0.1
$c_{\dot{d}}$, s^{-2}	−0.01
$c_{\ddot{d}}$, s^{-1}	−0.05

**Fig. 3** Time history of angle α for case 1: initial conditions from Eqs. (56) and (57).

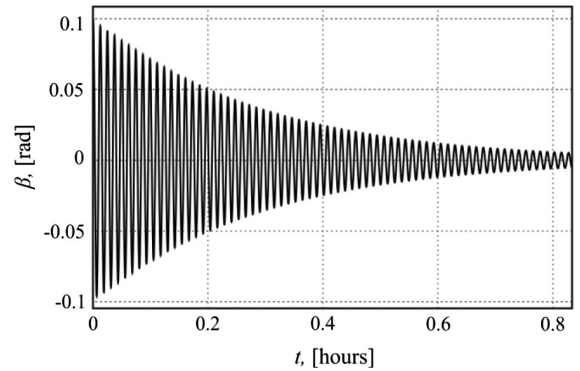
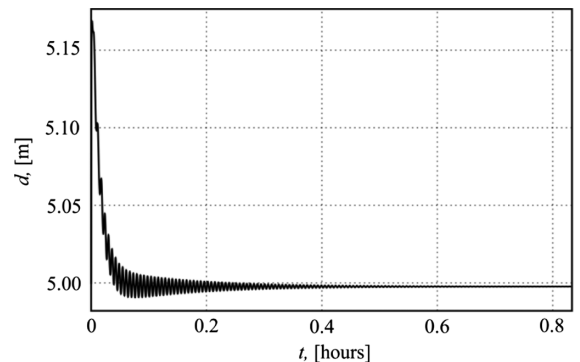
$$\theta_0 = \frac{\pi}{2}, \quad \dot{\theta}_0 = 0, \quad \eta = \frac{\pi}{2} \rightarrow G = \frac{K}{J} \cos \eta = 0 \quad (57)$$

Figures 3–5 depict the time dependence of the spherical angles α and β , and the distance between the space tug and debris d (Fig. 1) for the initial conditions stated through Eqs. (56) and (57). In this case, the pitch attitude angle $\theta = \theta_s = \pi/2$ and the charge of the space tug Φ_1 do not change.

From Figs. 3–5, it can be seen that the “ideal” initial conditions provide the stable, desired motion during the towing process of the debris.

Case 2: Nonideal initial conditions differ from the “ideal” Eqs. (56) and (57) when the line connecting the centers of mass C_1 and C_2 is perpendicular to the axis of symmetry of the debris $\theta_0 = \pi/2$ and not perpendicular to the vector of angular momentum (Fig. 2)

$$\eta = 1.3708 \quad (58)$$

**Fig. 4** Time history of angle β for case 1: initial conditions from Eqs. (56) and (57).**Fig. 5** Time history of the distance between the bodies for case 1: initial conditions from Eqs. (56) and (57).

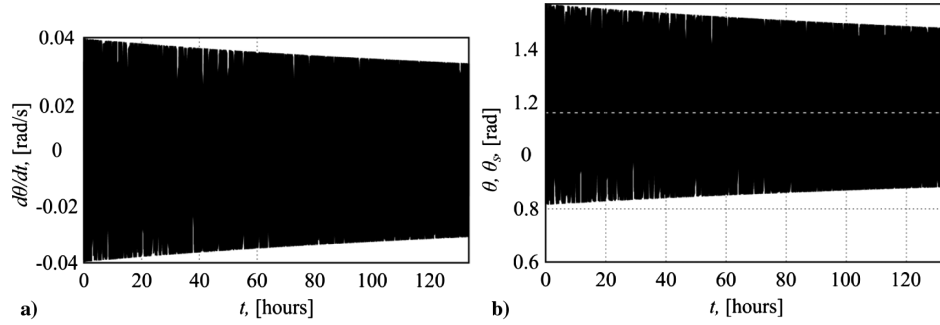


Fig. 6 Time history of pitch angle θ and angular velocity $d\theta/dt$ for case 2: initial conditions from Eqs. (56) and (60).

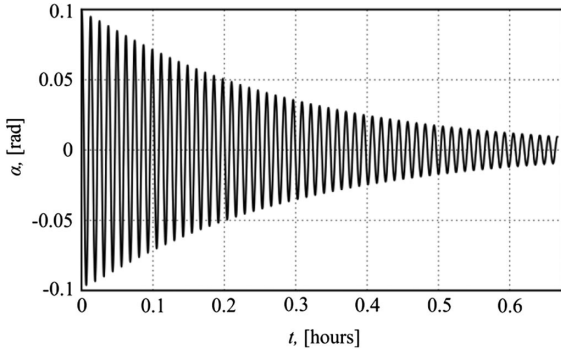


Fig. 7 Time history of angle α for case 2: initial conditions from Eqs. (56) and (60).

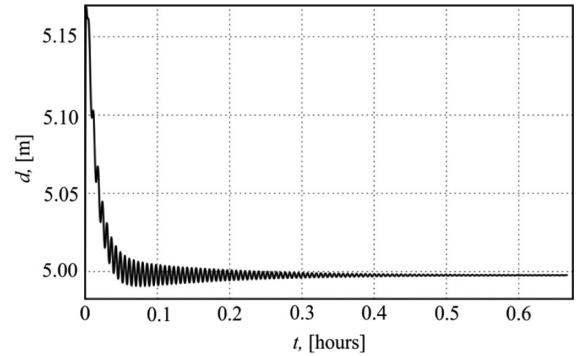


Fig. 9 Time history of the distance between the bodies d for case 2: the initial conditions (56) and (60).

The stable equilibrium position θ_s of the spatial motion is defined as the root of Eq. (45) for the known parameters R , G , and b . Equation (49) for gives $G = 0.04 \text{ s}^{-1}$. Then the root of Eq. (45) is

$$\theta_s = 1.1615 \quad (59)$$

The differential Eq. (45) is integrated with the following initial conditions:

$$\theta_0 = \frac{\pi}{2}, \quad \dot{\theta}_0 = 0 \quad (60)$$

Figures 6–10 show the time dependence of the pitch attitude angle θ , the spherical angles α and β , the distance between the space tug and debris d (Fig. 1), and the charge of the space tug Φ_1 for the initial conditions (56–60).

Figures 7–9 show the rapid stabilization of the motion parameters of the mass center of the debris relative to the tug, as in case 1. The damping process of the pitch angle θ to the equilibrium position $\theta_s = 1.1615$ occurs rather slowly (Fig. 6a). Figure 6b represents that the pitch angular velocity lies within $(-0.04, 0.04) \text{ rad/s}$ or $(-2.4, 2.4) \text{ rad/min}$, which decreases with time in case 2. The same

can be said about the voltage, and at the beginning of the motion, the voltage is the initial value of more than 8 kV (Fig. 10).

Case 3: This case differs from the previous one in that the initial pitch attitude angle θ_0 is equal to the equilibrium value $\theta_s = 1.1615$:

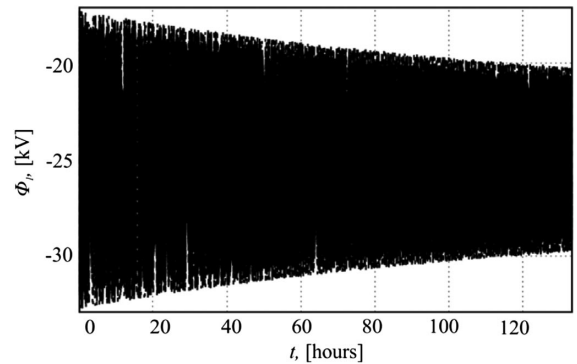


Fig. 10 Time history of the electrical charge of the tug $\Phi_1 = \Phi_1[1 + \kappa\theta \sin 2(\theta - \theta_s)]$ for case 2: initial conditions from Eqs. (56) and (60).

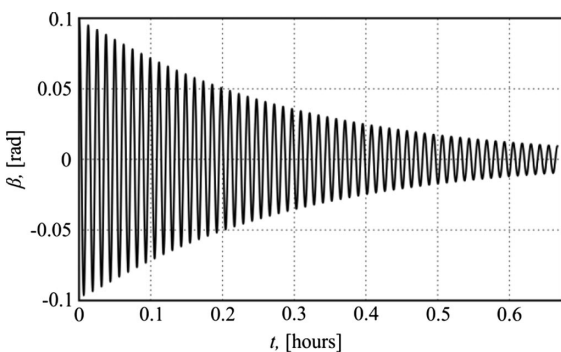


Fig. 8 Time history of angle β for case 2: initial conditions from Eqs. (56) and (60).

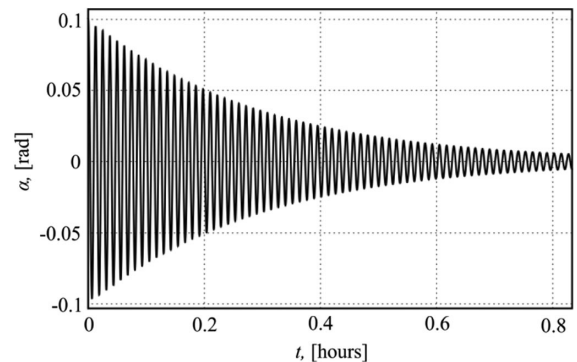


Fig. 11 Time history of angle α for case 3: initial conditions from Eqs. (56) and (61).

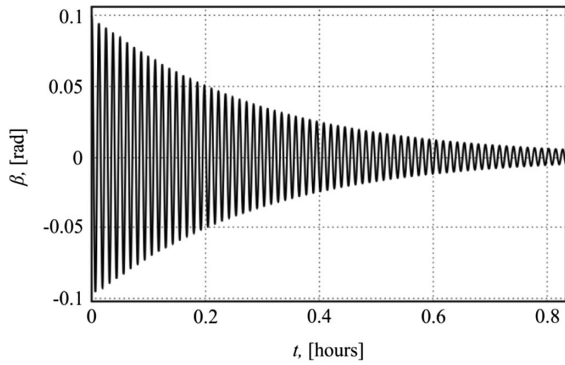


Fig. 12 Time history of angle β for case 3: initial conditions from Eqs. (56) and (61).

$$\theta_0 = \theta_s = 1.1615, \quad \dot{\theta}_0 = 0, \quad \eta = 1.3708 \rightarrow G = 0.04 \text{ s}^{-1} \quad (61)$$

Figures 11–13 depict the time dependence of the spherical angles α and β , and the distance between the space tug and debris d (Fig. 1) for the initial conditions stated through Eqs. (56–61). In this case, as well as in case 1, the pitch attitude angle $\theta = \theta_s = 1.1615$ and the charge of the space tug Φ_1 do not change.

Case 3 differs from case 1 only in that debris occupies not a perpendicular position relative to the line connecting the centers of mass of bodies, but at some angle $\theta = \theta_s = 1.1615$ (Figs. 11–13).

Case 4: Let us look at the configuration of the tug–debris system when the separation distance decreases to be of same order as the debris scale. We assume that the required distance between the tug and debris is

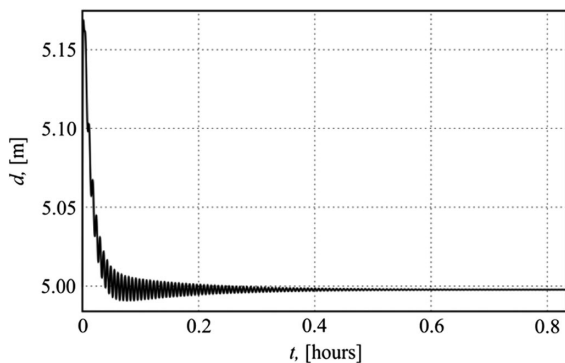


Fig. 13 Time history of the distance between the bodies d for case 3: initial conditions from Eqs. (56) and (61).

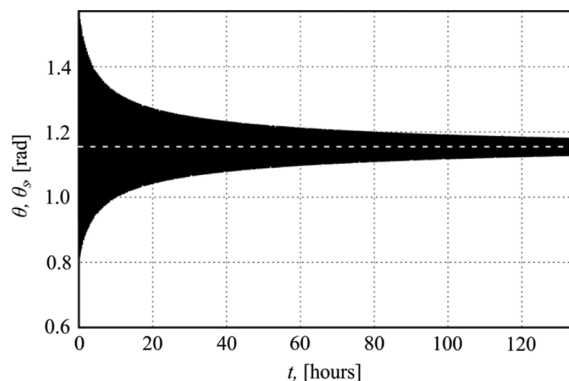


Fig. 14 Time history of pitch angle θ for case 4: initial conditions from Eqs. (56) and (60).

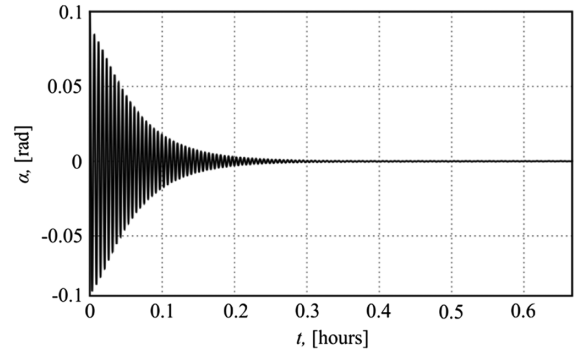


Fig. 15 Time history of angle α for case 4: initial conditions from Eqs. (56) and (60).

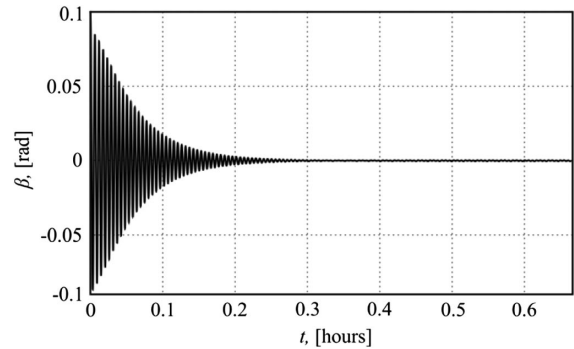


Fig. 16 Time history of angle β for case 4: initial conditions from Eqs. (56) and (60).

$$d_s = 1 \text{ m} \quad (\lambda_s = l/d_s = 0.5) \quad (62)$$

Obviously, condition (27) is not satisfied in this case. For numerical simulation, all other system parameters are selected from Tables 1 and 2. The initial conditions taken are the same as for case 2, that is, from Eqs. (56) and (60).

It is clear that if condition (27) is not satisfied, then the simplified Eqs. (38–42) cannot be used to simulate the motion. In this case the basic motion Eqs. (21–23), (10), (11) with the control law (32) should be used to numerical integration and study the system behavior.

Figures 14–18 illustrate the effectiveness the proposed feedback control laws in maintaining the desired position of the tug–debris system for case 4, when the separation distance decreases to be of same order as the debris scale.

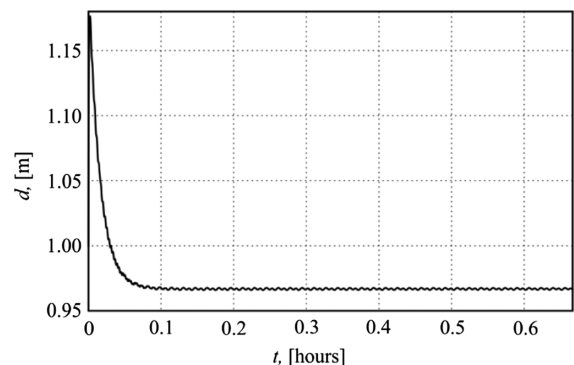


Fig. 17 Time history of the distance between the bodies d for case 4: initial conditions from Eqs. (56) and (60).

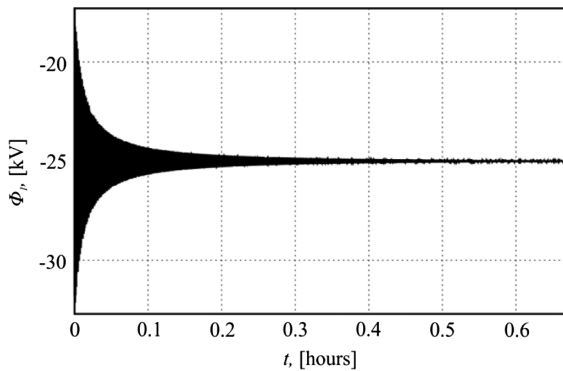


Fig. 18 Time history of the electrical charge of the tug $\Phi_1 = \Phi_1[1 + \kappa\theta \sin 2(\theta - \theta_s)]$ for case 4: initial conditions from Eqs. (56) and (60).

VII. Conclusions

This research explores the 3-D relative motion and debris spin rate stability of a pusher electrostatic tug configuration. The feature of this study is that it considers the spatial attitude motion of the debris as a rigid body relative to its own center of mass.

A simplified electrostatic force and torque formulation is employed to perform a numerical stability analysis for motions. It is analytically shown and numerically confirmed that the spatial attitude motion of the debris by electrostatic interaction in principle differs from the plane motion. Lagrange's interpretation is used to describe the spatial motion of debris as a rigid body, and an original mathematical model of the motion is proposed based on it. The peculiarity of the proposed mathematical model lies in the comparative simplicity on the one hand, and on the other hand, the ability to take into account the main features of the spatial motion. Based on a detailed analytical analysis of this model, the effect of the initial configuration of the tug–debris system on the spatial motion of the debris is shown, and it is proved that the stable position of the motion, to a large extent, depends on the initial position of the tug relative to the debris and the vector of the angular momentum of the debris. Practical recommendations are given on the formation of the initial configuration of the tug–debris system, which leads this system to the required motion. The numerical simulations illustrate the predicted relative motion and tumble rate stability for a range of tug force configurations, illustrating the robustness to such control parameter variations.

Acknowledgment

This work was supported by the Russian Science Foundation, Project No. 19-19-00085.

References

- [1] Liou, J.-C., Johnson, N., and Hill, N., "Controlling the Growth of Future LEO Debris Populations with Active Debris Removal," *Acta Astronautica*, Vol. 66, Nos. 5–6, 2010, pp. 648–653. doi:10.1016/j.actaastro.2009.08.005
- [2] Bonnal, C., Ruault, J.-M., and Desjean, M.-C., "Active Debris Removal: Recent Progress and Current Trends," *Acta Astronautica*, Vol. 85, April–May 2013, pp. 51–60. doi:10.1016/j.actaastro.2012.11.009
- [3] Anderson, P. V., and Schaub, H., "Local Debris Congestion in the Geosynchronous Environment with Population Augmentation," *Acta Astronautica*, Vol. 94, No. 2, Feb. 2014, pp. 619–628. doi:10.1016/j.actaastro.2013.08.023
- [4] Binz, C. R., Davis, M. A., Kelm, B. E., and Moore, C. I., "Optical Survey of the Tumble Rates of Retired GEO Satellites," *Advanced Maui Optical and Space Surveillance Technologies Conference*, Vol. 1, Curran Associates Inc., New York, 2014, p. 61.
- [5] Bombardelli, C., and Pelaez, J., "Ion Beam Shepherd for Contactless Space Debris Removal," *Journal of Guidance, Control, and Dynamics*, Vol. 34, No. 3, May–June 2011, pp. 916–920. doi:10.2514/1.51832
- [6] Kumar, R., and Sedwick, R. J., "Despinning Orbital Debris Before Docking Using Laser Ablation," *Journal of Spacecraft and Rockets*, Vol. 52, No. 4, 2015, pp. 1129–1134. doi:10.2514/1.A33183
- [7] Phipps, C. R., and Bonnal, C., "A Spaceborne, Pulsed UV Laser System for Re-Entering or Nudging LEO Debris, and Re-Orbiting GEO Debris," *Acta Astronautica*, Vol. 118, Jan.–Feb. 2016, pp. 224–236. doi:10.1016/j.actaastro.2015.10.005
- [8] Schaub, H., and Moorero, D. F., "Geosynchronous Large Debris Reorbiter: Challenges and Prospects," *Journal of the Astronautical Sciences*, Vol. 59, Nos. 1–2, 2014, pp. 161–176. doi:10.1007/s40295-013-0011–8
- [9] Hogan, E., and Schaub, H., "Relative Motion Control for Two-Spacecraft Electrostatic Orbit Corrections," *Journal of Guidance, Control, and Dynamics*, Vol. 36, No. 1, Jan.–Feb. 2013, pp. 240–249. doi:10.2514/1.56118
- [10] Aslanov, V., and Yuditsev, V., "Motion Control of Space Tug During Debris Removal by a Coulomb Force," *Journal of Guidance, Control, and Dynamics*, Vol. 41, No. 7, 2018, pp. 1476–1484. doi:10.2514/1.G003251
- [11] Aslanov, V., and Schaub, H., "Detumbling Attitude Control Analysis Considering an Electrostatic Pusher Configuration," *Journal of Guidance, Control, and Dynamics*, Vol. 42, No. 4, April 2019, pp. 900–9009. doi:10.2514/1.G003966
- [12] Aslanov, V., "Dynamics of a Satellite with Flexible Appendages in the Coulomb Interaction," *Journal of Guidance, Control, and Dynamics*, Vol. 41, No. 2, 2018, pp. 565–572. doi:10.2514/1.G002832
- [13] Aslanov, V., "Exact Solutions and Adiabatic Invariants for Equations of Satellite Attitude Motion Under Coulomb Torque," *Nonlinear Dynamics*, Vol. 90, No. 4, 2017, pp. 2545–2556. doi:10.1007/s11071-017-3822-5
- [14] Schaub, H., and Junkins, J. L., *Analytical Mechanics of Space Systems*, AIAA Education Series, 2nd ed., AIAA, Reston, VA, Oct. 2009, Chap. 14.
- [15] Stevenson, D., and Schaub, H., "Multi-Sphere Method for Modeling Electrostatic Forces and Torques," *Advances in Space Research*, Vol. 51, No. 1, Jan. 2013, pp. 10–20. doi:10.1016/j.asr.2012.08.014
- [16] Hogan, E. A., and Schaub, H., "Attitude Parameter Inspired Relative Motion Descriptions for Relative Orbital Motion Control," *Journal of Guidance, Control, and Dynamics*, Vol. 37, No. 3, 2014, pp. 741–749. doi:10.2514/1.60626
- [17] Schaub, H., and Stevenson, D., "Prospects of Relative Attitude Control Using Coulomb Actuation," *Journal of Astronautical Sciences*, Vol. 60, No. 3, 2013, pp. 258–277. doi:10.1007/s40295-015-0048-y
- [18] Hughes, J., and Schaub, H., "Spacecraft Electrostatic Force and Torque Expansions Yielding Appropriate Fidelity Measures," *AAS Spaceflight Mechanics Meeting*, Univelt Inc., San Diego, CA, 2017.
- [19] Wittenburg, J., *Dynamics of Multibody Systems*, 2nd ed., Springer-Verlag, Berlin, 2008, p. 233.